336
7-11-80

DOE/ET/20279-93
Distribution Category UC-63d

ANALYTICAL PREDICTION OF THE PERFORMANCE OF AN AIR PHOTOVOLTAIC/THERMAL FLAT-PLATE COLLECTOR

30 April 1980

P. Raghuraman

MASTER

Massachusetts Institute of Technology
Lincoln Laboratory
Lexington, Massachusetts 02173

Prepared For
THE U.S. DEPARTMENT OF ENERGY
UNDER CONTRACT NO. DOE/ET/20279

Additional copies available from the National Technical Information Service, U.S. Department of Commerce, Springfield, Virginia 22161.

Price: Paper Copy $4.00
Microfiche $3.00

DOE/ET/20279-93

ANALYTICAL PREDICTION OF THE PERFORMANCE OF AN AIR PHOTOVOLTAIC/THERMAL FLAT-PLATE COLLECTOR

30 April 1980

P. Raghuraman

Massachusetts Institute of Technology
Lincoln Laboratory
Lexington, Massachusetts 02173

Prepared For

THE U.S. DEPARTMENT OF ENERGY
UNDER CONTRACT NO. DOE/ET/20279

THIS PAGE

WAS INTENTIONALLY

LEFT BLANK

Abstract

A one-dimensional analysis developed by M.I.T. Lincoln Laboratory predicts the electrical and thermal performance of an air photovoltaic/thermal flat-plate collector. The analysis compares well with test measurements, predicting the thermal efficiency to within 2 percent. From the analysis, the poor thermal performance of the collector is attributable, in part, to the large undulations of the cell/silicone pottant surface in contact with the flowing air that results in less effective convective heat-transfer areas between the cell and the air.

THIS PAGE

WAS INTENTIONALLY

LEFT BLANK

CONTENTS

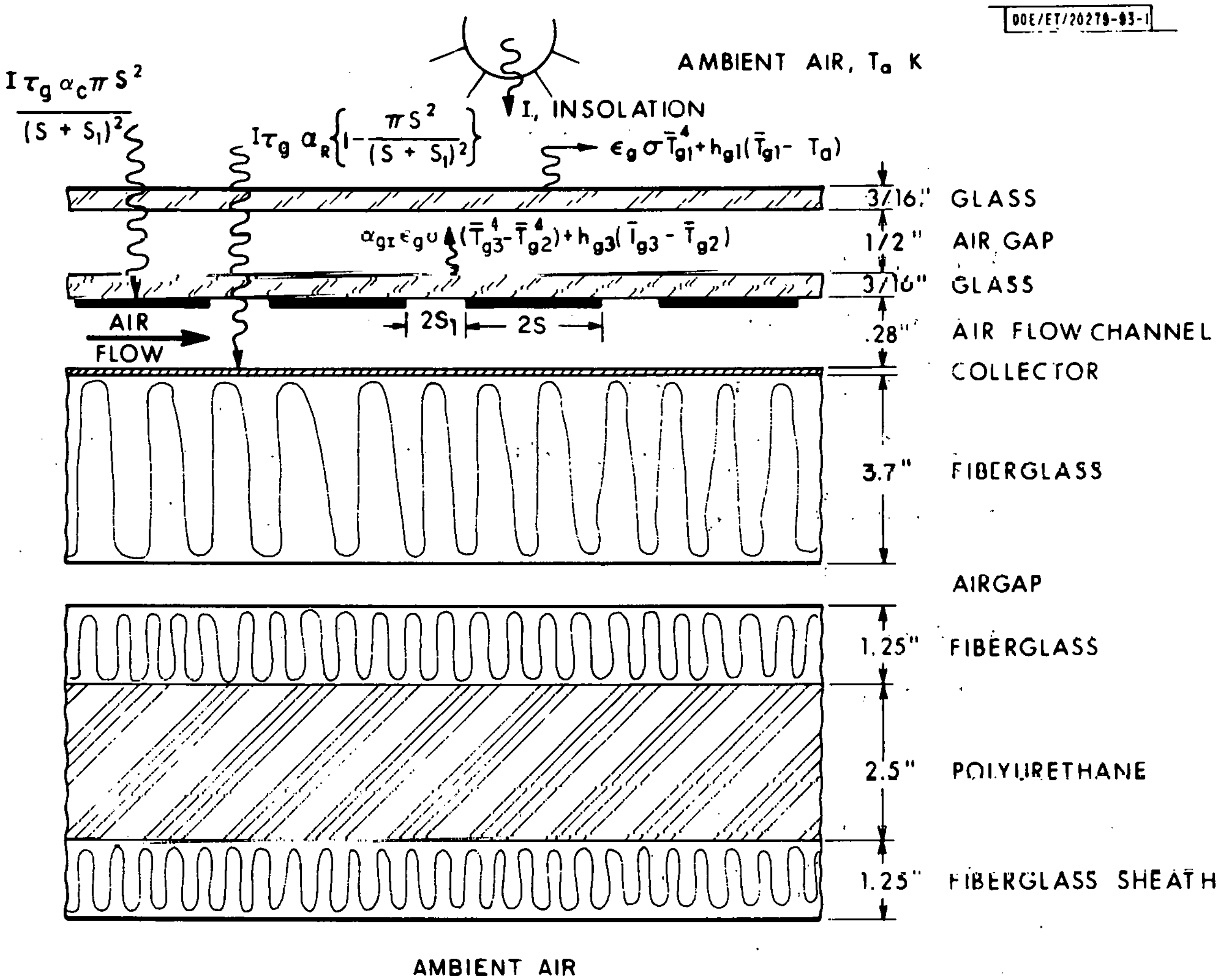

Fig. 1. Air photovoltaic/thermal collector cross section.

ANALYTICAL PREDICTION OF THE PERFORMANCE OF AN AIR PHOTOVOLTAIC/THERMAL FLAT-PLATE COLLECTOR

Introduction

Combined photovoltaic/thermal (PV/T) flat-plate collectors provide an attractive alternative to simple thermal or photovoltaic solar energy conversion. This report describes a numerical method to predict the thermal and electrical performance of one such collector, an air PV/T collector, currently under test at Lincoln Laboratory (Fig. 1). The collector consists of two glass covers with photovoltaic cells mounted on the underside of the inner glass cover. The cells, circular in shape are the primary absorber of the incident insolation. A black aluminum plate placed below the air-flow channel receives insolation passing between the cells. A sufficient amount of thermal insulation on the back of the plate keeps back-heat losses small.

Test measurements on the PV/T collector have been obtained at both Sandia Laboratories by Biringer and Smith[1] and at Lincoln Laboratory by Hendrie.[2] Analytical solutions to simple thermal collector performance are available from the classical analysis of Hottel and Whillier[3] and have since been extended to PV/T collectors by Florschuetz.[4] In Florschuetz's analysis, the solar cells are tacitly assumed to have a 100-percent packing efficiency. Further, the cells and absorber plate are modeled as a uniform temperature composite. In the PV/T collector, the packing efficiency is 63 percent, and a 0.28-inch air gap separates the bottom of the cell from the collector plate. It is therefore not evident that Florschuetz's analysis is directly applicable to the air PV/T collector. In fact, Florschuetz's analysis, together with the use of Klein's overall collector loss coefficient,[5] overestimates the measured thermal efficiency by as much as 10 percent. This report extends Florschuetz's analysis to the PV/T collector where the packing efficiency is less than 100 percent and the cells are at a different temperature from the collector. The analysis developed has the added feature of being functions of the various collector component heat-transfer coefficients: radiation, conduction, and convection. Several of the radiative heat-transfer parameters were obtained by direct measurements. This analysis can, therefore, be used in making a parametric study of the collector constituents and its influence on the collector performance.

The next Section describes the model and the relevant equations used. The last Section compares the result of the analysis with teat measurements and infers some conclusions on the design of the collector.

Formulation and Assumption of Model

Heat-transfer processes in the collector are represented pictorially in Fig. 1. The model used follows closely that of Hottel. It neglects edge losses and it consists of one-dimensional heat-transfer processes that are described in the next two subsections.

1. Collector Overall Heat Transfer

Insolation, I, is transmitted through the two glass covers (transmissivity = τ_g, absorptivity = 0), part of which is absorbed by circular cell surfaces (absorptivity-to-visible light = α_c) while the fraction transmitted between the cells is absorbed by the thermal absorber plate. The cell diameter, 2S = 3 inches, is large compared to spacing between them, $2S_1$ = 0.1 inch. The absorptance-to-visible light is large for the cell (0.89) and the thermal collector (α_R = 0.88). Therefore, neglecting interreflection of insolation between the cell and glass covers and the cell and thermal absorber plate, the average insolation absorbed by the cells and thermal receiver per unit cell/glass area are $I\tau_g\alpha_c p$ and $I\tau_g\tau_p\alpha_R(1 - p)$, respectively. Here p is the cell packing factor (based on cell envelope area) defined as $\pi S^2/(S + S_1)^2$, while τ_g is the transmittance-to-visible light of the pottant filling the space between cells.

If η_e is the cell electrical efficiency, then $I\tau_g\alpha_c\eta_e p$ is the electrical energy produced per unit area of the cell/glass interface, while the balance, $I\tau_g\alpha_c(1 - \eta_e)p$, is released by the cell as thermal energy. This energy is partly lost by conduction to the top of the lower glass cover, $K_g(\bar{T}_c - \bar{T}_{g3})/d_g$, where $\bar{T}_c$, $\bar{T}_{g3}$ are the average temperatures of the cell/pottant composite and top surface of lower glass plate while K_g, d_g are the glass thermal conductivity and thickness. The conducted thermal energy is transferred to the top glass cover by natural convection and/or conduction, $h_{g3}(\bar{T}_{g3} - \bar{T}_{g2})$, and by radiation, $\alpha_{gI}\epsilon_g\sigma(\bar{T}^4_{g3} - \bar{T}^4_{g2})$. Here $\bar{T}_{g3}$ and $\bar{T}_{g2}$ are the bottom (upper surface) and top glass (lower surface) temperatures, h_{g3} the natural convection and/or conduction coefficient between glass covers, and α_{gI} and ϵ_g are the infrared absorptance and emission of glass. Inter-reflection of infrared radiation between the glass covers is neglected as α_{gI} is close to unity. The heat transfer in the air gap is purely conductive for small air-gap thicknesses; with increasing air-gap thicknesses, natural convection in the air gap becomes the dominating heat-transfer mode. Following Buchberg, et al.[5], the convective heat-transfer coefficient, h_{g3}, is given as:

$$\frac{h_{g3}d}{K_A} = 0.157\ Ra_d^{0.285} \quad \text{for } Ra_d > 20000$$
$$= 1 \quad \text{for } Ra_d < 1700 \quad .$$

Here, d and K_A are the air-gap thickness and thermal conductivity, and Ra_d is the Rayleigh number based on d.

Thermal energy is then conducted through to the top glass cover surface, $K_g(\bar{T}_{g1} - \bar{T}_{g2})/d_{g1}$, from where it is radiated out, $\epsilon_g \sigma \bar{T}_{g1}^4$, and convected away, $h_g(\bar{T}_{g1} - T_a)$. Here, d_{g1} is the top glass cover thickness, $\bar{T}_{g1}$ the glass cover temperature, T_a the ambient temperature, and h_g the glass cover convective heat-transfer coefficient. Following Stultz and Wen,[6] h_g is available as:

$$h_g = 1.247\left[(\bar{T}_{g1} - T_a)\cos\theta\right]^{1/3} + 2.685V$$

where h_g has the units, Watt/m^2 ^{o}K; the temperatures are in ^{o}C, and the wind velocity, V, is in m/sec. θ is the module inclination to the horizontal. Radiation from the sky to the top glass cover is given by $\alpha_{gI}\sigma(T_a - 3)^4$ where $T_a - 3$ is assumed to be the sky temperature.

The balance of the thermal energy released by the cell is convected away by the flowing air, Q_c, and partly radiated to the thermal collector plate, $\alpha_{RI}\epsilon_c\sigma\bar{T}_c^4 - \alpha_{cI}\epsilon_R\sigma\bar{T}_R^4$, while the plate, in turn, transfers energy to the flowing air by convection, Q_R. Here $\bar{T}_R$ is the average thermal collector plate temperature, and h_c is the convective heat-transfer from the cell/pottant composite to the flowing air; ϵ_R, α_{RI}, and ϵ_c, α_{cI} are the emissivity and infrared absorptance of the thermal collector and cell/pottant, respectively. Here, inter-reflection of infrared radiation between the cells and thermal collector has been neglected since α_{RI} and α_{cI} are close to unity. Heat is lost from the thermal collector plate through the back insulation to the atmosphere. This loss is neglected in this analysis. On the basis of the results thus obtained, it is estimated that this would result in overestimating the collector thermal efficiency by less than 1 percent.

Translating to equations:

$$I\tau_g\alpha_c(1 - \eta_e)p = Q_c + \frac{K_g}{d_g}(\bar{T}_c - \bar{T}_{g3}) + \alpha_{RI}\epsilon_c\sigma\bar{T}_c^4 - \alpha_{cI}\epsilon_R\sigma\bar{T}_R^4 \quad , \tag{1}$$

$$I\tau_g\tau_p\alpha_R(1 - p) + \alpha_{RI}\epsilon_c\sigma\bar{T}_c^4 = Q_R + \alpha_{cI}\epsilon_R\sigma\bar{T}_R^4 \tag{2}$$

$$\frac{K_g}{d_g}(\bar{T}_c - \bar{T}_{g3}) = \alpha_{gI}\epsilon_g\sigma(\bar{T}_{g3}^4 - \bar{T}_{g2}^4) + h_{g3}(\bar{T}_{g3} - \bar{T}_{g2}) \tag{3}$$

$$\frac{K_g}{d_g}(\bar{T}_c - \bar{T}_{g3}) = \frac{K_g}{d_{g1}}(\bar{T}_{g2} - \bar{T}_{g1}) \tag{4}$$

and

$$\frac{K_g}{d_{g1}}(\bar{T}_{g2} - \bar{T}_{g1}) = \epsilon_g\sigma\bar{T}_{g1}^4 + h_g(\bar{T}_{g1} - T_a) - \alpha_{gI}\sigma(T_a-3)^4 \tag{5}$$

These equations carry the tacit assumption that the air gaps are thin enough to make them optically thin to radiation passing through them. The cell electrical efficiency is modeled by a linear relation:

$$\eta_e = \eta_{eR}\,[1 - \eta'(\bar{T}_c - T_{ref})]$$

where η_{eR}, η' and T_{ref} are constants whose values are found in Appendix A. These are five equations in five unknowns: $\bar{T}_{g1}$, $\bar{T}_{g2}$, $\bar{T}_{g3}$, $\bar{T}_c$, and $\bar{T}_R$, and can be solved for if the heat transfer from the cells and the thermal collector plate, Q_c,Q_R are known. These are obtained in the next subsection.

2. Temperature Distribution in Flow Direction

Let T_f be the mass averaged air temperature in the channel, $\dot{m}$ the mass flow rate, and c_p the specific heat of air. The change in T_f along the channel length is then related to q_c and q_R, the local heat flux to the air from the cells and the thermal collector plate by:

$$\dot{m} c_p \frac{dT_f}{dx} = w\,(q_c + q_R) \tag{6}$$

where x is the coordinate along the channel length and w is channel width. q_c and q_R can be expressed as:

$$q_c = h_c\,(\bar{T}_c - T_f) \tag{7}$$

$$q_R = h_R\,(\bar{T}_R - T_f) \tag{8}$$

where h_c and h_R are the convective heat-transfer coefficients of the cell wall and the thermal collector plate. Here, the effect of axial heat conduction on the cell/glass and thermal collector plate (opposite to flow direction) is neglected. Following Kays[8] where the value for the Nusselt number for fully developed laminar velocity and temperature profiles between parallel plates is tabulated, it is assumed that h_c and h_R are given by:

$$\frac{h_c\, 2d_A}{K_A} = \alpha\, 7.54$$
$$\frac{h_R\, 2d_A}{K_A} = 7.54 \tag{9}$$

where K_A, d_A are the thermal conductivity and height of the air in the channel, and α is a constant whose value can range from 0 to 1. It is used to incorporate the fact that the cell surface has large undulations normal to the air flow that could have a detrimental effect on the heat transferred to air by the cell surface.

Substituting Eqs. (7) and (8) in Eq. (6) and integrating across the channel length, ℓ, for the final air temperature, T_{fo}, yields:

$$T_{fo} = \left\{ T_{fi} - \frac{(h_c\bar{T}_c + h_R\bar{T}_R)}{h_c + h_R} \right\} \exp\left[\frac{-(h_c + h_R)\,\ell w}{\dot{m} c_p} \right] + \frac{h_c\bar{T}_c + h_R\bar{T}_R}{h_c + h_R} \tag{10}$$

where T_{fi} is the incoming air temperature. The average heat transfer per unit channel length to the air flow from the cell surface and the thermal collector plate, Q_c, Q_R, to be used in Eqs. (1) and (2) can be evaluated as:

$$Q_i = \frac{1}{\ell}\int_0^{\ell} dx\ q_i \qquad i = c,\ R$$

to yield

$$Q_j = h_j \left\{ T_j - \frac{(h_c\bar{T}_c + h_R\bar{T}_R)}{h_c + h_R} - \frac{\dot{m}c_p}{(h_c+h_R)\ell w}\left[T_{fi} - \frac{(h_c\bar{T}_c + h_R\bar{T}_R)}{h_c+h_R}\right]\exp\left[\frac{-\ell w(h_c+h_R)}{\dot{m}c_p}\right]\right\}$$

$$j = c,\ R \qquad (11)$$

The collector thermal and electrical efficiencies are then defined, respectively, as:

$$\eta_T = \frac{\dot{m}c_p}{IA_T}(T_{fo} - T_{fi})$$

and

$$\eta_{e\ell} = \eta_e \frac{N\pi S^2}{A_T}$$

where A_T = Overall module area

N = Total number of cells in the module.

Equations (11) together with (1)–(5) constitute seven equations in seven unknowns and are solved on the computer. The approach used in solving these equations was to assume a value of Q_c, solve for various temperatures, and check to see if it yields the assumed value Q_c. A Newton-Raphson iteration technique is used to yield the values of the seven unknowns. Typically, the solution converges in about six iterations.

The various parameters used in the calculations are listed in Appendix A. Some have been obtained from tables, while some, specifically the radiative coefficients, were measured.

Results

Figures 2 and 3 show the theoretical electric and thermal efficiency for the air PV/T module. Superimposed are the experimental results. Calculations were done for $I = 1\ kw/m^2$, $T_a = 295^oK$, $\alpha = 0.5$, and varying values of T_{fi}. The analysis predicts both the electrical and thermal efficiency quite accurately. Thermal efficiencies were calculated both with and without electrical power and differ from test measurements by less than 2 percent. More importantly, the slope of the thermal efficiency curves, which is a measure of the collector overall loss coefficient, is simulated quite accurately by the analysis.

Figure 4 is again a comparison of calculated thermal efficiencies with test measurements for the same parameters as in Fig. 3, except that two values of α, 1.0 and 0.5, are used. The thermal performance of the collector, can be increased by about 10 percent by improving the heat transfer between the cell and air flow. A visual examination of the cell/pottant surface (using photographs) reveal a large amount of undulations in the surface normal to the air flow directions. These undulations lead to large recirculating flow regions, resulting in reduced heat transfer between the air flow and the cell.

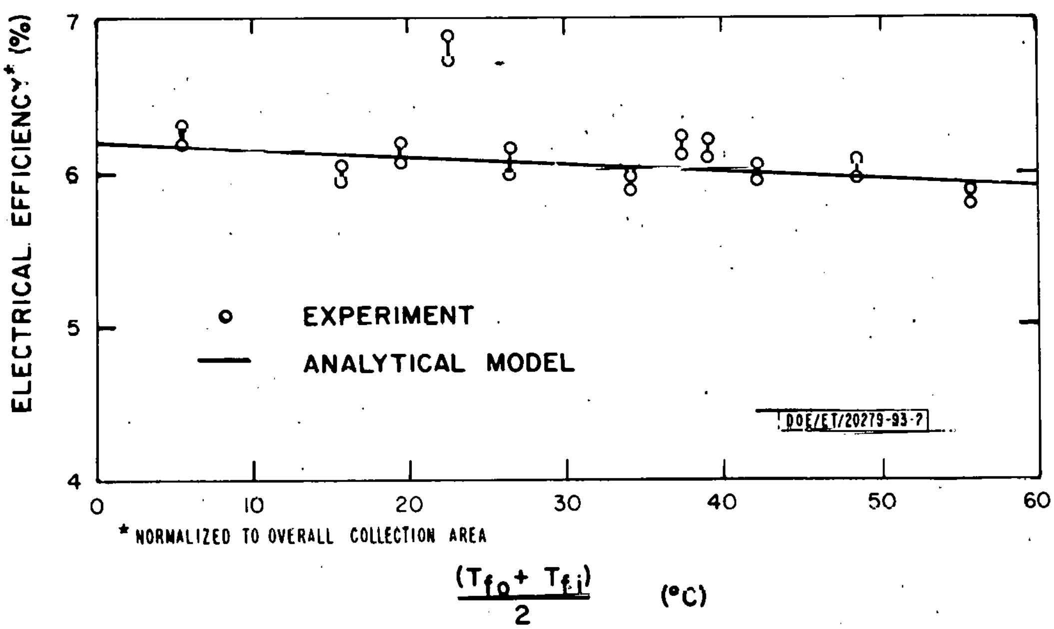

Fig. 2. Electrical measurements: Analysis vs. test measurements.

Fig. 3. Module thermal efficiency, comparison of analysis and test measurements.

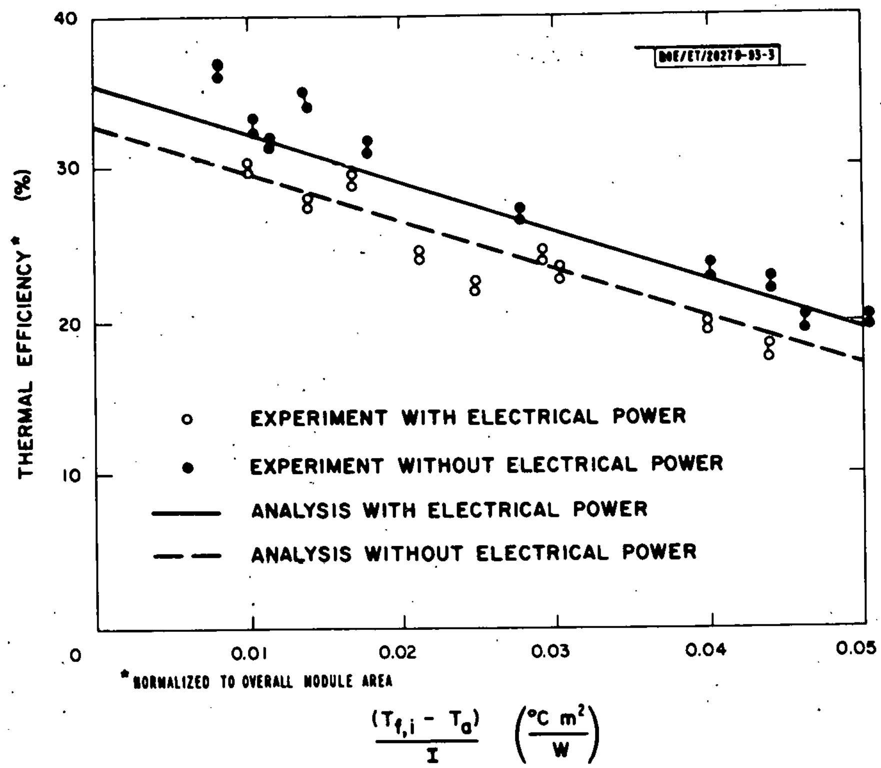

Fig. 4. Effect of α on the module thermal efficiency.

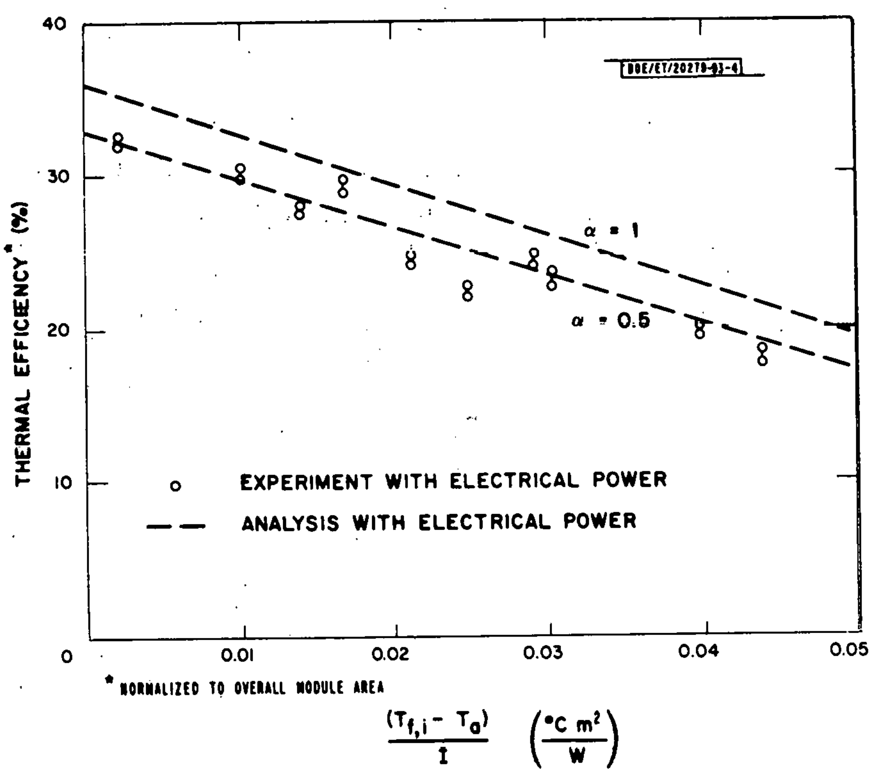

Conclusions

An analysis that is an extension of Florschuetz's analysis, has been developed for a PV/T air collector. The analysis indicates that a marginal improvement in the thermal efficiencies can be anticipated by eliminating large undulations on the cell/pottant surface.

Future PV/T collectors could yield higher thermal efficiencies by the following modifications:

a. Heat losses through the top cover glass to the ambient air is made up of, typically, 60-percent radiative and 40 percent of convective losses. Convective losses may be reduced, it is conjectured, by a series of crisscrossing grooves on the top glass cover. These grooves aid in the formation of recirculation zones in the ambient air flowing over the surface, and therefore, reduce the effective convective heat-transfer coefficient of the glass surface.

b. Elimination of large undulations on the cell/pottant surface normal to the flow direction.

c. The air flow through the channel is laminar. Trip wires on the walls normal to the air flow can be used to make it turbulent. Further, both the absorber plate and cell/pottant surface can be made rough to enhance heat transfer. Also, fins along the flow direction will increase heat transfer.

d. The limited data of Buchberg, et al.[5], suggests that there exists an optimum, cell-to-glass cover air-gap height for which the thermal conductance-to-heat loss is a minimum. This height is critically dependent on the cell-to-glass temperature difference. For the calculated temperature difference of 8° to $17^{\circ}C$, corresponding to insolation values between 50 to

100 mw/cm^2, this height is greater than 5 cm as opposed to 1.27 cm in the design tested. This change is expected to reduce top losses by over 10 percent.

e. The thermal resistance between the cells and the air flow must be kept as small as possible. This can be done by minimizing the epoxy thickness on the cells. The traditional epoxy-silicone RTV has a thermal conductivity, K, of 0.002 watts/cm ^{o}C. However, several high-thermal conductive, high-dielectric-strength, high-transmissivity epoxies are available with K ranging from 0.008 to 0.016 watts/cm ^{o}C. Use of these epoxies in place of the silicone pottant, would ensure a low thermal resistance between the cells and air flow while ensuring electrical insulation.

The following are two additional devices, whose cost-effectiveness is in question, to increase the thermal and electrical performance of the PV/T collector:

a. Use of anti-reflective coatings on the top surfaces of the two glass covers. These coating are made of magnesium fluoride and bismuth oxide and reduce reflection of insolation substantially.

b. Use of selective black coatings of black nickel or chrome on the thermal collector plate. These coatings are almost perfect absorbers of insolation and have a very low emissivity.

References

1. K. L. Biringer and D. R. Smith, "Development and Testing of Combined Photovoltaic/Thermal Flat-Plate Collectors," American Sect. International Solar Energy Society (1978).

2. S. D. Hendrie, "Evaluation of Combined Photovoltaic/Thermal Collectors," International Solar Energy Society, Atlanta, Georgia (28 May – 1 June 1979).

3. H. C. Hottel and A. Whillier, "Evaluation of Flat-Plate Solar Collector Performance," The Scientific Basis, II, Pt. 1, Sect. A, 74-104 (University of Arizona Press, Tuscon, Arizona, 1958).

4. L. W. Florschuetz, "Extension of the Hottel-Whillier Model to the Analysis of Combined Photovoltaic/Thermal Flat-Plate Collector," Solar Energy, 22, 361-366 (1979).

5. H. Buchberg, I. Catton, and D. K. Edwards, "Natural Convection in Enclosed Spaces: A Review of Application to Solar Energy Applications," ASME 74-WA/HT-12 (New York 1974).

6. J. W. Stultz and L. C. Wen, "Thermal Performance Testing and Analysis of Photovoltaic Modules in Natural Sunlight," LSSA Project Task Report 5101-31, Jet Propulsion Laboratory, California Institute of Technology (29 July 1977).

7. W. M. Kays, Convective Heat and Mass Transfer, 117 (McGraw-Hill, New York, 1960).

Appendix A

A Gier Dunkle model MS3 reflectometer for visible light was used together with a backing (for transparent surfaces) of mirror or a black surface, to measure the absorptivity and transmissivity of various surfaces to visible light. A model DB100 Gier Dunkle reflectometer for infrared light was also used to meaure the emissivity of various surfaces. The result of the measurements are:

• Glass cover absorptivity (visible light)	0
• Transmissivity through two glass covers	0.86
• Glass cover emittance	0.87
• Cell absorptance (visible light)	0.89
• Cell emittance	0.92
• Silicone pottant transmissivity	0.72
• Thermal collector absorbance to visible light	0.88
• Thermal collector emittance	0.87

Other parameter values used:

• Glass thickness	0.48 cm
• Air space thickness	1.27 cm
• Air channel height	0.7 cm
• Air channel width	85 cm
• Air channel length	153 cm
• Cell diameter	7.6 cm
• Cell spacing	0.250 cm
• Glass absorptance to infrared radiation	1.0
• Cell absorptance to infrared radiation	0.87
• Thermal collector absorbance to infrared radiation	0.87
• Thermal conductivity of air	0.00027 W/cm ^{o}C
• Thermal conductivity of glass	0.009 W/cm ^{o}C
• η_{eR}	0.117
• η'	0.0022

• T_{ref}	$318^{o}K$
• Module inclination	55 degrees
• Wind velocity	2.2 m/sec
• Air mass flow rate	0.0186 kg/sec
• Viscosity of air	0.000018 kg/msec
• Prandtl number for air	0.7
• Specific heat for air	1012 Joules/kg ^{o}C
• Total number of cells in module	216
• Overall module area	1.55 m^2